Tert-butylamidinate tin(II) complexes: high activity, single-site initiators for the controlled production of polylactide†‡§

Nonsee Nimitsiriwat,[a] Vernon C. Gibson,*[a] Edward L. Marshall,*[a] Andrew J. P. White,[a] Sophie H. Dale[b] and Mark R. J. Elsegood[b]

Received 3rd May 2007, Accepted 17th July 2007
First published as an Advance Article on the web 9th August 2007
DOI: 10.1039/b706663e

The tin(II) coordination chemistry of two monoanionic *N*,*N*′-bis(2,6-diisopropylphenyl)alkylamidinate ligands is described. Complexation studies with the acetamidinate, $[MeC(NAr)_2]^-$, (Ar = 2,6-^{i}Pr$_2$C$_6$H$_3$) are complicated by the side formation of the bis(amidinate) tin(II) compound, $[MeC(NAr)_2]_2Sn$, **1**. By contrast, the bulkier *tert*-butylamidinate, $[^tBuC(NAr)_2]^-$, allows tin(II) mono-halide, -alkoxide and -amide complexes to be isolated cleanly in high yields. Thus, the reaction of $[^tBuC(NAr)_2]H$ with ^{n}BuLi and subsequent treatment with $SnCl_2$ generates $[^tBuC(NAr)_2]SnCl$, **2**, in *ca.* 70% yield. Reactions of **2** with LiO^{i}Pr, $LiNMe_2$ and $LiNTMS_2$ afford $[^tBuC(NAr)_2]Sn(O^iPr)$, **3**, $[^tBuC(NAr)_2]Sn(NMe_2)$, **4**, and $[^tBuC(NAr)_2]Sn(NTMS_2)$, **5**, respectively. The molecular structures of complexes **1–4** are reported. Complexes **3**, **4** and **5** have been investigated as initiators for the ring-opening polymerisation of *rac*-lactide: **3** and **4** display characteristics of well-controlled polymerisation initiators, but high molecular weight polymer is observed with **5** due to inefficient initiation, a consequence of the steric bulk of the $NTMS_2$ unit. Polymerisations with **3** and **4** are faster than for the corresponding β-diketiminate tin(II) complexes, consistent with the more open nature of the tin(II) coordination sphere.

Introduction

The replacement of petrochemically derived products with biomass based alternatives is exemplified by the commercial synthesis of poly(lactide), PLA, from starch.[1,2] Industrially, tin(II) bis(2-ethylhexanoate), $SnOct_2$, is employed as the polymerisation initiator because it is soluble and thermally stable in molten lactide, thereby allowing the process to be conducted in the melt phase in the absence of organic solvents.

Numerous metal alkoxides are known to initiate polymerisation of lactide, LA[3–5] and although details of the mechanism by which $SnOct_2$ functions remain ambiguous, in the presence of alcohol the propagating species is commonly believed to be a tin(II) alkoxide.[6–10] In order to synthesise single-site, well-defined analogues of $SnOct_2$ we have therefore previously reported the β-diketiminate tin(II) alkoxide complex, $[HC\{C(Me)N\text{-}2,6\text{-}^iPr_2C_6H_3\}_2]Sn(O^iPr)$, and shown that it polymerises *rac*-LA in a well-controlled manner.[11,12] Although slower than comparable complexes of more electropositive metals (*e.g.* Zn,[13–15] Mg,[15,16] Ca[17,18] and Fe[19]), improved activities were obtained with less hindered and with halogenated β-diketiminates, as anticipated for a coordinative-insertion mechanism.[12]

However, we also observed an unusual stereochemical invariance among the PLA samples prepared using this initiator family: a wide range of β-diketiminate tin(II) initiators all afforded PLA with a similar heterotactic bias. Computational analysis led us to propose that this behaviour arises from a reluctance of the 5s lone pair to mix with other Sn orbitals. The orientation of bound monomer relative to the propagating polymer chain is therefore determined principally by the need to interact with the tin centre through orthogonally aligned pd hybrids, relegating the steric and electronic properties of the β-diketiminate ligand to a secondary role.

We thus decided to target amidinate ligands containing *N*,*N*′-2,6-diisopropylphenyl substituents for two major reasons. Firstly, we envisaged that amidinate[20,21] ligands would give more accessible metal centres than their corresponding β-diketiminates, potentially allowing improved catalytic activities to be realised (Scheme 1). Secondly, we also wanted to investigate whether opening up the coordination sphere whilst retaining the same aryl substituents would lead to a change in stereocontrol. Here therefore, we describe the synthesis of tin(II) complexes of *N*,*N*′-bis(2,6-diisopropylphenyl) alkylamidinate ligands and compare

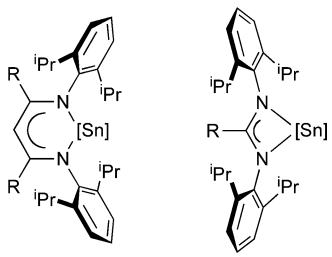

Scheme 1

[a]*Department of Chemistry, Imperial College London, South Kensington Campus, London, UK SW7 2AZ. E-mail: v.gibson@imperial.ac.uk, e.marshall@imperial.ac.uk*
[b]*Chemistry Department, Loughborough University, Loughborough, Leicestershire, UK LE11 3TU*

† The HTML version of this article has been enhanced with colour images.

‡ CCDC reference numbers 645832–645835. For crystallographic data in CIF or other electronic format see DOI: 10.1039/b706663e

§ Electronic supplementary information (ESI) available: Crystallographic data for complex **1** and details of kinetic studies using complex **3**; Fig. S1–S7. See DOI: 10.1039/b706663e

lactide polymerisation behaviour with their β-diketiminate analogues.

Results and discussion

Synthetic studies

Our initial investigations were performed using the acetamidine, $[MeC(NAr)_2]H$, Ar = 2,6-$^{i}Pr_2C_6H_3$.[22] However, all attempts to synthesise tin(II) complexes of this ligand resulted in the co-generation of the bis(amidinate) complex, $[MeC(NAr)_2]_2Sn$, **1**. For example, lithiation of the acetamidine and subsequent addition to $SnCl_2$ resulted in a mixture of the desired $[MeC(NAr)_2]SnCl$ complex and **1** in a 2 : 3 ratio. Similarly, the reaction of $MeC(NAr)_2H$ with $Sn(NMe_2)_2$ in Et_2O afforded $[MeC(NAr)_2]Sn(NMe_2)$ contaminated with *ca.* 20–25% **1**. The more bulky diamide $Sn(NTMS_2)_2$ reacted very slowly with $MeC(NAr)_2H$ at room temperature, and when the reaction was repeated at 80 °C overnight, an analytically pure sample of **1** was obtained (Scheme 2).

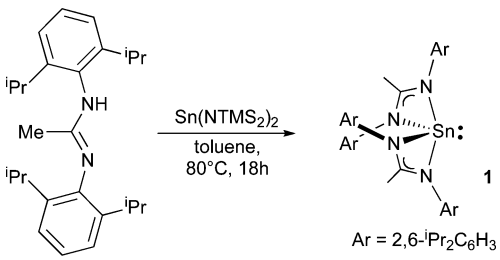

Scheme 2

X-Ray diffraction analysis of **1** revealed the presence of two independent C_2-symmetric molecules (**I** and **II**) with essentially identical geometries (molecule **I** is shown in Fig. 1, molecule **II** in Fig. S2 in the ESI§). Though highly distorted, the coordination geometry can be viewed as saw-horse like, with N(2) and N(2A) in the axial positions, and N(1) and N(1A) residing in the equatorial plane. Consistent with the use of 5p4d hybrid frontier orbitals, many of the interligand angles at tin approach 90° [N(1)–Sn–N(1A) = 101.33(12); N(1)–Sn–N(2A) = N(2)–Sn–N(1A) = 97.98(8)°]. This structure is analogous to several previously reported tin(II) bis(amidinate)s[23–28] and is therefore not discussed in further detail.

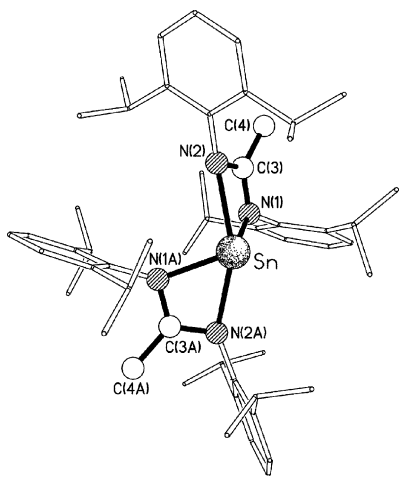

Fig. 1 The molecular structure of one (molecule **I**) of the two independent C_2-symmetric molecules present in the crystals of **1**. The suffix 'A' indicates the equivalent positions $(1 - x, y, \frac{1}{2} - z)$.

Whilst *N,N′*-silyl[26,27] and *N,N′*-cyclohexyl[24] bis(amidinate) tin(II) compounds exhibit a single set of N-substituent NMR resonances at 298 K, axial and equatorial sites of complex **1** do not readily exchange at room temperature. Hence, eight equally intense methyl doublets and three isopropyl methine septets (in the ratio 2 : 1 : 1) are observed in its ^{1}H NMR spectrum. Such behaviour is attributed to the steric bulk of the N-aryl units in **1**, with coalescence of the ^{i}Pr resonances only occurring at elevated temperature (348 K). The tetra-coordinate nature of the metal in the solid state is retained in solution as shown by a singlet ^{119}Sn NMR resonance at −394.8 ppm, notably upfield of signals for the three coordinate species described below (which occur between +50 and −30 ppm).

In light of the ease with which the bis(amidinate) **1** forms, we concluded that the {$[MeC(NAr)_2]Sn$(II)} fragment is unlikely to prove a suitable stabilising unit for single-site polymerisation systems. We therefore turned our attention to the complexation chemistry of the analogous *tert*-butylamidinate ligand.[29] Jordan and co-workers have previously shown that a *tert*-butyl group on the amidinate carbon forces the N-substituents to project further towards the metal[30] and we rationalised that this might serve to suppress bis(chelate) formation in our system, while still affording markedly less steric protection than β-diketiminate ligands.

In situ lithiation of $[^{t}BuC(NAr)_2]H$ using $^{n}BuLi$ followed by addition to a toluene suspension of $SnCl_2$ afforded the tin(II) monochloride complex, $[^{t}BuC(NAr)_2]SnCl$, **2** in *ca.* 70% yield following recrystallisation from heptane (Scheme 3). No evidence for the presence of the bis(amidinate) analogue of **1** was observed in either the crude reaction product or in the recrystallised material.

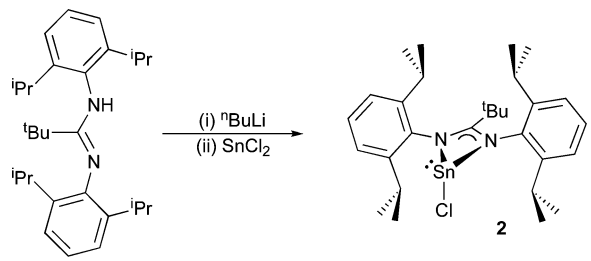

Scheme 3

X-Ray diffraction quality crystals of **2** were obtained by allowing a saturated heptane solution to cool slowly from 70 °C to ambient temperature. The molecular structure (Fig. 2) is similar to that of $[^{t}BuC(NAr)_2]GeCl$[31] with the tin centre adopting a three-coordinate distorted pyramidal geometry. Hybridisation of the metal 4d and 5p orbitals is supported by the near perpendicular alignment of the Sn–Cl vector to the amidinate ligand (N(1)–Sn–Cl = 94.93(4), N(2)–Sn–Cl = 94.89(4)°). The anionic charge on the ligand is clearly delocalised over the amidinate backbone as shown by the symmetric bonding pattern within the core (N(1)–C(1) = 1.3418(19), N(2)–C(1) = 1.3374(19) Å; N(1)–Sn = 2.2022(13), N(2)–Sn = 2.2104(13) Å). The tin atom is essentially coplanar with the amidinate (sum of the internal angles of the CN_2Sn core = 359.91°), whilst N(1), N(2) and C(1) all approach trigonal planarity as anticipated for sp^2 hybridisation, with the sum of the

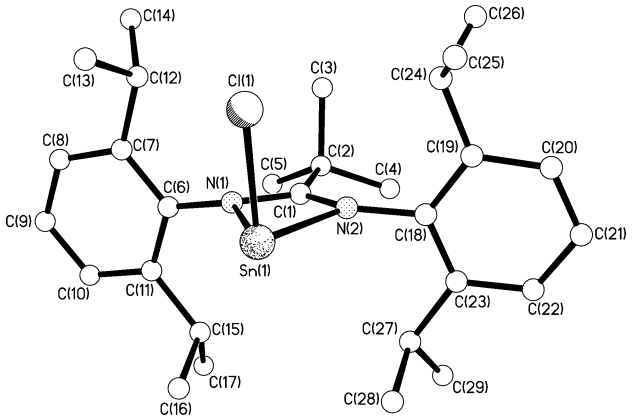

Fig. 2 The molecular structure of complex **2**.

angles around these three atoms being 357.82, 358.94 and 359.60° respectively. The acute N–Sn–N angle of 59.40° is comparable to values previously recorded for tin(II)[23–28] and tin(IV)[32,33] amidinate complexes. The aryl rings are aligned in a near-orthogonal manner relative to the ligand chelate plane, and the N–C_{ipso} bonds are orientated out of the CN_2Sn plane in a *syn* fashion, causing the two isopropyl moieties below the amidinate chelate plane to lie significantly closer together than the pair on the opposite face (distances between C(15) and C(27) = 4.11, C(12) and C(24) = 5.71 Å). The less sterically congested face of the complex is therefore used to accommodate both the chloride ligand and one of the *tert*-butyl methyl groups (torsional angle between C(2)–C(3) and Sn–Cl = 0.2°).

To examine further the extent of the steric protection afforded the metal centre by the *tert*-butylamidinate ligand we have compared the structure of **2** to that of a β-diketiminate counterpart, [HC{MeC(N-2,6-^{i}Pr$_2$C$_6$H$_3$)}$_2$]SnCl, which has previously been reported by Roesky, Power and co-workers.[34] As shown in Fig. 3, the β-diketiminate ligand evidently encapsulates both the tin atom and the chloride ligand more effectively than the amidinate unit.

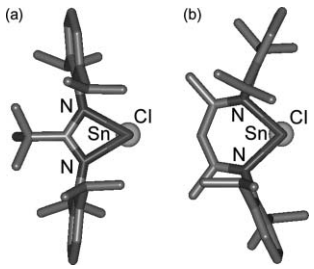

Fig. 3 Comparison of the solid states structures of (a) complex **2** with (b) [HC{MeC(N-2,6-^{i}Pr$_2$C$_6$H$_3$)}$_2$]SnCl viewed along the Sn–Cl vector (H atoms omitted for clarity).

The ^{1}H NMR (C_6D_6) spectrum of **2** indicates that its solid state structure is maintained in solution. The *tert*-butyl group on the ligand backbone obstructs rotation of the aryl rings on the NMR timescale, with two distinct isopropyl resonance patterns observed (C*H*Me$_2$ septets: δ 4.06, 3.48; CH*Me*$_2$ doublets: d 1.47, 1.31, 1.26, 1.07).

Complex **2** serves as a convenient precursor to alkoxide and amide complexes (Scheme 4). For example, its reaction with LiO^iPr cleanly generates [^{t}BuC(NAr)$_2$]SnO^iPr, **3**. This observation

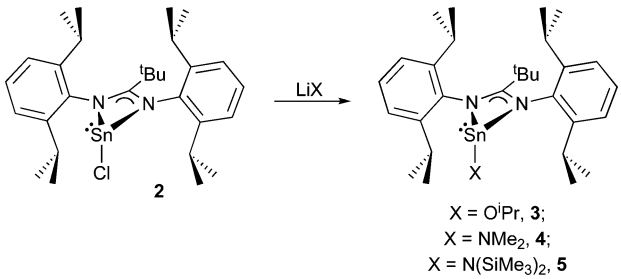

Scheme 4

contrasts markedly with a previous study of less bulky N-silyl benzamidinate ligands, with only exceptionally bulky alkoxide tin(II) complexes proving isolable.[27]

The ^{1}H NMR spectrum of **3** at 298 K is similar to that of **2**, although some broadening of the aryl resonances is observed (including unresolved multiplets for H_{meta} and H_{para}, and two broad septets and four broad doublets for the $CHMe_2$ groups). The resonances of the isopropoxide ligand, and of the amidinate *tert*-butyl substituent are all sharp, suggesting that in solution at room temperature these units are free to rotate, but their steric bulk serves to restrict rotation of the aromatic rings about the N–C_{ipso} vectors.

Complex **3** (Fig. 4) is essentially isostructural to **2**: the tin atom again displays a distorted pyramidal geometry and is coplanar with the three amidinate ring atoms (sum of internal angles in the CN_2Sn core = 359.55°). Geometries at N(1), N(2) and C(1) are consistent with sp^2-hybridisation (sum of angles = 358.27, 357.45 and 359.85° respectively). The separation between the isopropyl methine carbons C(12) and C(24) is 5.59 Å, 1.33 Å greater than the distance between C(15) and C(27), and the alkoxide oxygen is located in a similar position to the chloride of complex **2**, with an average N–Sn–O bond angle of 93.8°.

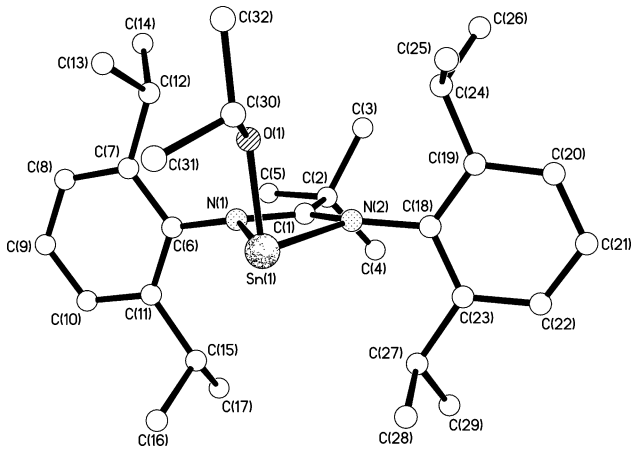

Fig. 4 The molecular structure of complex **3**.

Treatment of complex **2** with $LiNMe_2$ and with $LiNTMS_2$ affords the mononuclear amides [^{t}BuC(NAr)$_2$]SnNR_2 (R = Me, **4**; R = $SiMe_3$, **5**), again with no bis(amidinate) contamination. A further repercussion of the increased size of the ancillary ligand became apparent when we tried to synthesise **5** by reaction of the *tert*-butylamidine with Sn(NTMS_2)$_2$: no reaction was observed even after heating to 80 °C in toluene for 70 h.

Table 1 Selected bond parameters for **1–4**

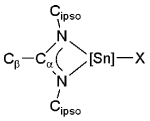

	1 (mol **I**)	**2**	**3**	**4**
Bond lengths/Å				
C_α–N	1.343(3)	1.3418(19)	1.345(2)	1.354(2)
	1.314(3)	1.3374(19)	1.338(2)	1.331(2)
Sn–N	2.444(2)	2.2104(13)	2.2216(15)	2.2600(15)
	2.197(2)	2.2022(13)	2.2085(15)	2.2401(16)
Sn–X	—	2.4282(6)	2.0056(14)	2.0414(18)
Bond angles/°				
C_α–N–Sn	97.80(17)	95.68(9)	95.93(11)	95.77(11)
	87.59(16)	95.44(9)	95.09(11)	95.53(11)
N–Sn–N′	57.13(8)	59.40(5)	59.21(5)	58.38(6)
N–C_α–N′	114.1(2)	109.37(13)	109.32(15)	109.66(16)
N–Sn–X	—	94.93(4)	94.37(5)	99.42(7)
	—	94.89(4)	93.27(6)	99.36(6)
C_α–N–C_{ipso}	121.7(2)	131.95(13)	132.72(15)	131.64(16)
	119.9(2)	131.93(13)	132.32(15)	130.57(16)
Sn–N–C_{ipso}	145.61(18)	131.57(10)	130.46(11)	129.90(12)
	133.96(18)	130.19(10)	129.20(11)	127.32(12)
C_β–C_α–N	123.1(2)	125.00(13)	126.34(16)	126.54(16)
	122.8(2)	125.23(13)	124.19(15)	123.51(16)

The molecular structure of **4** (Fig. 5) also features a distorted pyramidal tin(II) centre and amidinate bond parameters similar to those found in the structures of **2** and **3** (pertinent data for **1–4** are summarised in Table 1). Notably, the angles N(1)–Sn–N(3) and N(2)–Sn–N(3) (99.36 and 99.42°, respectively) are *ca.* 5–6° greater than those in **2** and **3**, reflecting the increased steric bulk of the NMe_2 unit relative to the Cl and O^{i}Pr ligands.

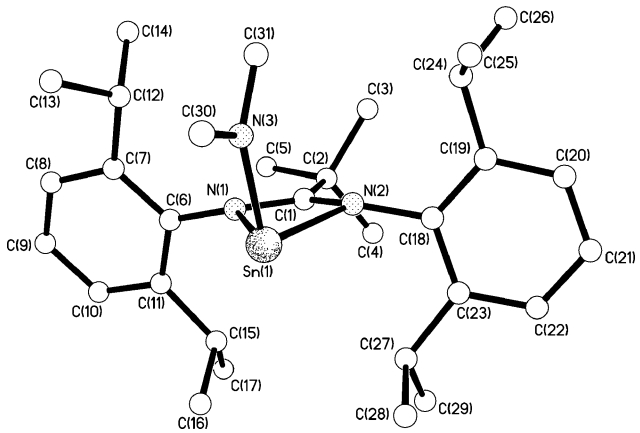

Fig. 5 The molecular structure of complex **4**.

Polymerisation of *rac*-lactide

In order to study the behaviour of the alkoxide **3** and the amides **4** and **5** as lactone ring-opening polymerisation initiators, each complex was mixed with 100 equivalents of *rac*-LA in toluene at 60 °C, *i.e.* under the same conditions examined for β-diketiminate tin(II) initiators.[11,12] Aliquots were then removed over the course of the polymerisation and monomer conversion and molecular weight were determined by ^{1}H NMR and GPC, respectively.

As shown in Fig. 6, complex **3** is a well-controlled polymerisation initiator: a plot of M_n *versus* monomer conversion is linear, and molecular weight distributions are narrow, although a slight deviation from linearity is observed at high conversions (>85%) indicative of an increased prevalence for transesterification as the monomer concentration declines.[35]

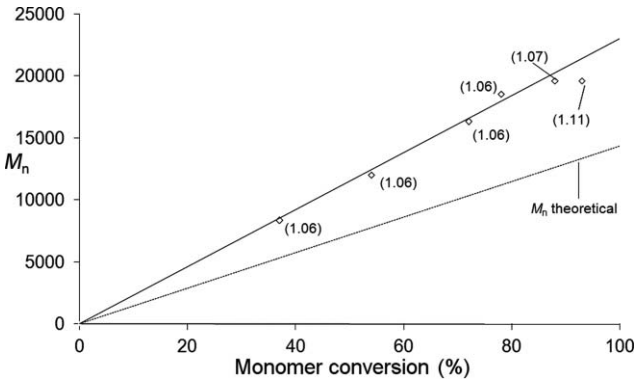

Fig. 6 A plot of M_n *vs.* monomer conversion for the polymerisation of *rac*-LA using complex **3** as the initiator ([LA] : [**3**] = 100; 60 °C; toluene; polydispersities given in parentheses).

A linear relationship is also observed between M_n and $[LA]_0/[\mathbf{3}]$ (Fig. S4, ESI§). The polymerisation of *rac*-LA using **3** as an initiator is further characterised by a first-order dependence upon monomer concentration, as demonstrated by a linear correlation between $\ln\{[LA]_0/[LA]_t\}$ and reaction time (Fig. 7). However, repeating this analysis over a range of initiator concentrations ($1.4–3.5 \times 10^{-2}$ mol L^{-1}), revealed a non-first-order dependence upon [**3**]. Examining the variation of rate with initiator concentration indicates that the polymerisation adheres to the rate law $-d[LA]/dt = k[LA][\mathbf{3}]^{0.21}$ (*i.e.* a rate law order dependence on [**3**] of just 0.21; see ESI§). Thus, with [LA] kept constant and the concentration of **3** varied so as to give initial [LA]/[**3**] ratios of 80, 100, 133 and 200, after 60 min conversions reached 83%, 78%, 75% and 72%, respectively. This result contrasts with our findings on the β-diketiminate analogue, [HC{MeC(NAr)}$_2$]Sn(O^{i}Pr), which exhibits first-order kinetics.[12]

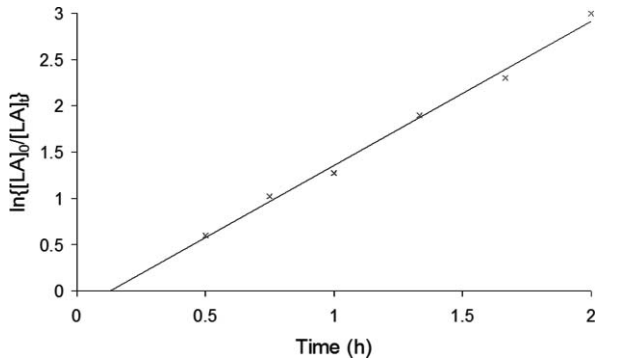

Fig. 7 A plot of $\ln\{[LA]_0/[LA]_t\}$ *vs.* time for the polymerisation of *rac*-LA using complex **3** as the initiator (60 °C; toluene; $[LA]_0 = 0.28$ M; [**3**] = 0.0014 M; $[LA]_0$: [**3**] = 200).

Fractional rate law orders of this type have been observed with other lactide polymerisation initiators;[27,36–39] in the most salient study, Aubrecht, Hillmyer and Tolman found a rate law dependence of 0.33 for an equimolar initiating mixture of $[PhC(NSiMe_2Ph)_2]Sn(OCPh_3)$ + $PhCH_2OH$ at 80 °C.[27] Low rate orders have traditionally been explained in terms of the structural reorganisation of the metal coordination sphere to give multinuclear aggregates. In the amidinate tin(II) system, however, we believe that aggregation is more likely to occur *via* the reversible coordination of the propagating polyester chains to the readily accessible active sites. Nevertheless, the polymerisation of *rac*-LA using **3** is still significantly faster than with the β-diketiminate initiators $[HC\{RC(NAr)\}_2]Sn(O^iPr)$ which typically require *ca.* 4 (R = Me) and 8 (R = ^{t}Bu) h at 60 °C to consume 100 equivalents of monomer (k_{app} = 0.734 and 0.384 h^{-1}, respectively).[5] By contrast, complex **3** attains similar levels of conversion within 90 min (k_{app} = 1.78 h^{-1}).

In order to examine the initiation process more closely, complex **3** was mixed with 5 equivalents of *rac*-LA in CD_2Cl_2 at 298 K and the reaction was monitored by ^{1}H NMR spectroscopy. As shown in Fig. 8, within just 15 min the initiator and one equivalent of monomer are cleanly converted into a new species, which in light of our previous study[12] is believed to be the first insertion product **6** (Scheme 5). Thereafter, the reactants remain unchanged for *ca.* 2 h, before gradual consumption of the monomer is observed. The rapid formation of **6** is signified by the disappearance of the

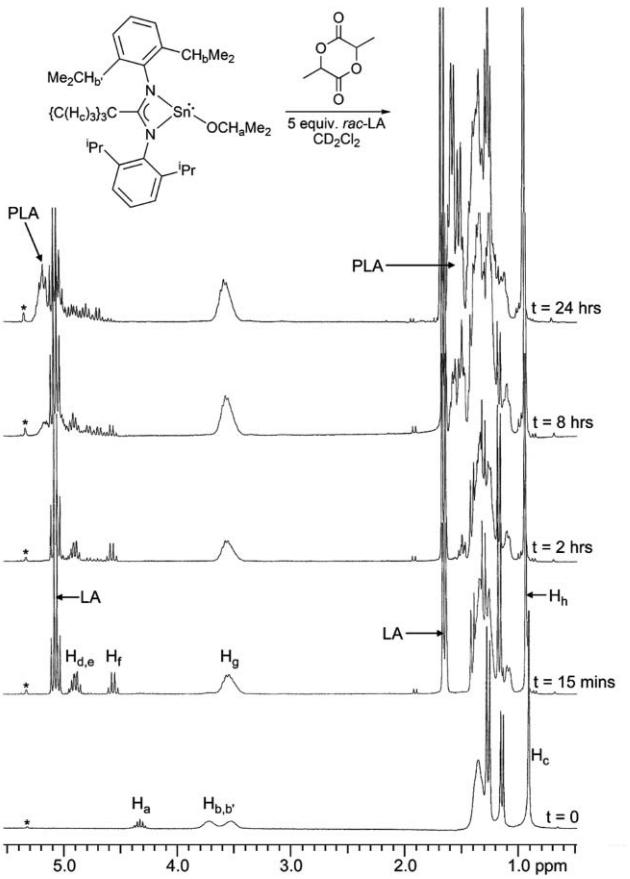

Fig. 8 ^{1}H NMR spectra of the reaction between **3** and 5 equivalents *rac*-LA (CD_2Cl_2, 298K, 250 MHz; * = $CHDCl_2$). Spectrum shown at t = 0 was recorded prior to monomer addition.

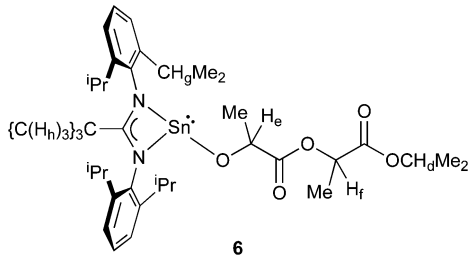

6

Scheme 5

tert-butyl H_c singlet at 0.85 ppm and the emergence of a new singlet at δ 0.91 (H_h). Other resonances associated with the newly formed compound include quartets at δ 4.88 and 4.57 (H_e and H_f), and the H_d septet at 4.90 ppm, indicative of the $CO_2{}^iPr$ end group. Initiation (*i.e.* formation of **6**) is therefore rapid, whereas the insertion of a second lactide molecule is far slower (Fig. 7 confirms that a short delay—*ca.* 8 min—also exists prior to polymerisation at 60 °C). Similar delays have been observed with the tin(II) diketiminate initiators and have recently been the focus of a theoretical study.[12]

The polymerisations of *rac*-LA initiated with **4** and **5** also demonstrate linearly proportional increases in molecular weight with monomer consumption (Fig. 9). However, whilst the dimethylamide complex **4** produces molecular weights similar to those recorded for the alkoxide initiator **3**, use of the more bulky bis(trimethylsilyl)amide **5** results in much higher molecular weights (and appreciably broader molecular weight distributions). For example, at 93% and 92% conversion, respectively, the M_n values of PLA synthesised using **3** and **4** are 19 600 and 20 700; by contrast, an M_n of 122 000 was recorded for PLA prepared from **5** at 91% LA consumption. We ascribe this observation to unfavourable initiation by the bulky $NTMS_2$ unit, leading to a smaller number of propagating chains than expected from the initial monomer : initiator stoichiometry. The slow rate of initiation also impacts upon the time taken for the polymerisations to attain high conversion. Hence, under the conditions employed, complex **3** consumes > 90% of 100 equivalents *rac*-LA within 90 min; similar levels of conversion with **4** and **5** require 180 and 240 min, respectively.

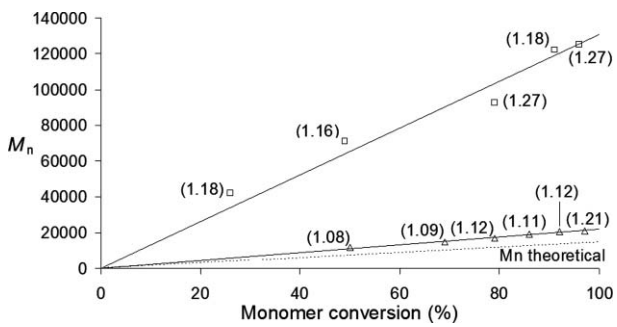

Fig. 9 A plot of M_n *vs.* monomer conversion for the polymerisation of *rac*-LA using complexes **4** (△) and **5** (□) as the initiator (60 °C; toluene $[LA]_0$: [**4**] = 100; $[LA]_0$: [**5**] = 100; polydispersities given in parentheses).

A moderate bias to heterotactic assembly[40] is observed with initiators **3–5**, as exemplified by Fig. 10. Similar levels of hetero-selectivity have been observed with many tin(II) initiators,[11,12,27] and our observations lend further support to computational studies[12]

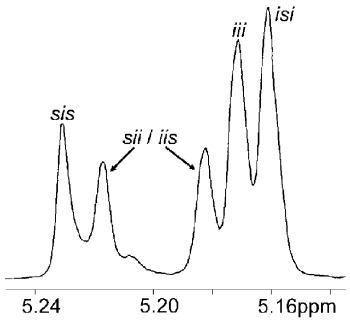

Fig. 10 The methine region of the ^{1}H decoupled NMR spectrum (298 K, 400 MHz, $CDCl_3$) of PLA prepared using complex **3** at 60 °C in toluene (i = isotactic, s = syndiotactic dyads).

which indicate that the tin $5s^2$ lone pair of electrons plays an instrumental role in determining stationary point geometries along the reaction coordinate.

Conclusion

The *N,N′*-bis(2,6-diisopropylphenyl)(*tert*-butyl) amidinate ligand allows tin(II) coordination chemistry to be explored without the complication of bis(chelate) side formation. X-Ray crystallography indicates that this ligand provides the metal centre with far less protection than its β-diketiminate counterpart, and *rac*-lactide polymerisations are accordingly faster, even though the activities are presumably tempered by aggregation. For complexes **3** and **4**, the increased reactivity is coupled with good molecular weight control, but the identity of the initiating group is a crucial factor: the much bulkier bis(trimethylsilyl)amide group initiates the polymerisation of *rac*-LA poorly, and high molecular weights result.

The tacticity of the PLA products are similar to those obtained using β-diketiminate tin(II) initiators (and $SnOct_2$[12]) giving strong support to our hypothesis that the presence of the $5s^2$ lone pair of electrons and the deployment of 4d5p hybrid orbitals exert an influence over the monomer ring-opening event much larger than the attendant ligand(s).

Experimental

General

All solvents were distilled over standard drying agents under nitrogen and were deoxygenated before use. $Sn(NMe_2)_2$,[41] $[MeC(NAr)_2]H$[22] and $[^tBuC(NAr)_2]H$[29] were prepared according to literature procedures. *Rac*-lactide was purchased from the Sigma Aldrich Chemical Co. and sublimed three times prior to use. All other chemicals were purchased from the Sigma Aldrich Chemical Co. and used as received.

NMR spectra were recorded on a Bruker DRX400 instrument. ^{1}H (400 MHz) and ^{13}C (100 MHz) NMR chemical shifts are quoted in ppm relative to the residual solvent resonances; ^{119}Sn (186.5 Hz) spectra were referenced to the internal standards of the machine. Microanalyses were carried out at the University of North London. GPC chromatograms were recorded using a Polymer Laboratories LC1220 HPLC pump and a Spark Midas autosampler connected to two 5 μm columns (300 × 75 mm) and a Shodex RI-101 differential refractometer. Chromatograms were analysed using Cirrus Software (Polymer Laboratories) and molecular weights are reported *versus* polystyrene calibrants.

Synthesis of $[MeC(NAr)_2]_2Sn$, 1

To a 30 mL toluene solution of $Sn\{N(TMS)_2\}_2$ (0.48 g, 1.09×10^{-3} mol) was added a 30 mL toluene suspension of $MeC(NAr)_2H$ (0.41 g, 1.09×10^{-3} mol) dropwise at room temperature. The reaction was stirred at 80 °C overnight. Solvent was distilled off under reduced pressure and the residue was washed with cold pentane and then dried to give $[MeC(NAr)_2]_2Sn$, **1**, as a pale yellow solid, (Found: C, 71.52; H, 8.55; N, 6.59%; $C_{52}H_{74}N_4Sn$ requires C, 71.47; H, 8.54; N, 6.41%); $\delta_H(C_6D_6)$ 7.30–7.07 (m, 12H, H_{meta}, H_{para}), 3.76 (br sept, 4H, $^3J_{HH} = 6.5$ Hz, $CH(CH_3)_2$), 3.33 (br sept, 2H, $^3J_{HH} = 6.7$ Hz, $CH(CH_3)_2$), 3.17 (br sept, 2H, $^3J_{HH} = 6.6$ Hz, $CH(CH_3)_2$), 1.57 (br d, 6H, $^3J_{HH} = 6.6$ Hz, $CH(CH_3)_2$), 1.48 (br d, 6H, $^3J_{HH} = 6.6$ Hz, $CH(CH_3)_2$), 1.38 (s, 6H, $(CH_3)C(NAr)_2$), 1.36 (overlapping br d, 6H, $CH(CH_3)_2$), 1.29 (br d, 6H, $^3J_{HH} = 6.7$ Hz, $CH(CH_3)_2$), 1.25 (br d, 6H, $^3J_{HH} = 6.8$ Hz, $CH(CH_3)_2$), 1.16 (br d, 6H, $^3J_{HH} = 6.6$ Hz, $CH(CH_3)_2$), 0.96 (br d, 6H, $^3J_{HH} = 6.7$ Hz, $CH(CH_3)_2$), 0.68 (br d, 6H, $^3J_{HH} = 6.7$ Hz, $CH(CH_3)_2$); $\delta_C(C_6D_6)$ 168.69 ($MeC(NAr)_2$), 145.09 (C_{ortho}), 144.75 (C_{ipso}), 143.88 (C_{ortho}), 142.71 (C_{ipso}), 141.81 (C_{ortho}), 141.48 (C_{ortho}), 125.71 (C_{para}), 124.93 (C_{para}), 124.41 (C_{meta}), 123.52 (C_{meta}), 123.26 (C_{meta}), 29.30 ($CHMe_2$), 28.81 ($CHMe_2$), 28.17 ($CHMe_2$), 27.46 ($CH(CH_3)_2$), 25.57 ($CH(CH_3)_2$), 25.26 ($CH(CH_3)_2$), 25.09 ($CH(CH_3)_2$), 24.59 ($CH(CH_3)_2$), 23.57 ($CH(CH_3)_2$), 23.40 ($CH(CH_3)_2$), 22.30 ($CH(CH_3)_2$), 16.64 ($(CH_3)C(NAr)_2$); $\delta_{119Sn}(C_6D_6)$ −394.77; m/z 713 ($M - (CH(CH_3)_2)_2C_6H_3$).

Synthesis of $[^tBuC(NAr)_2]SnCl$, 2

A suspension of $[^tBuC(NAr)_2]Li$ (9.55×10^{-3} mol) in 60 mL toluene (formed *in situ* from the reaction of ^{n}BuLi, 2.5 M in hexanes, with $[^tBuC(NAr)_2]H$) was added to $SnCl_2$ (1.813 g, 9.56×10^{-3} mol) in toluene (30 mL) at −78 °C. The reaction mixture was allowed to warm to room temperature and then stirred for 18 h. The yellow solution was filtered and volatiles removed to give a beige solid. This was recrystallised from heptane to give $[^tBuC(NAr)_2]SnCl$ as pale yellow crystals (3.781 g, 6.59×10^{-3} mol, 69% yield). Crystals suitable for X-ray crystallography were grown by slow cooling of a heptane solution from 70 °C to room temperature, (Found: C, 60.77; H, 7.33; N, 4.85%; $C_{29}H_{43}N_2SnCl$ requires C 60.70, H 7.55, N 4.88%); $\delta_H(C_6D_6)$ 7.12–6.97 (m, 6H, H_{meta}, H_{para}), 4.06 (sept, 2H, $^3J_{HH} = 6.7$ Hz, $CH(CH_3)_2$), 3.48 (sept, 2H, $^3J_{HH} = 6.8$ Hz, $CH(CH_3)_2$), 1.47 (d, 6H, $^3J_{HH} = 6.6$ Hz, $CH(CH_3)_2$), 1.31 (d, 6H, $^3J_{HH} = 6.9$ Hz, $CH(CH_3)_2$), 1.26 (d, 6H, $^3J_{HH} = 6.9$ Hz, $CH(CH_3)_2$), 1.07 (d, 6H, $^3J_{HH} = 6.8$ Hz, $CH(CH_3)_2$), 0.88 (s, 9H, $C(CH_3)_3$); $\delta_C(C_6D_6)$ 180.01 ($^tBuC(NAr)_2$), 145.64 (C_{ortho}), 143.53 (C_{ortho}), 140.23 (C_{ipso}), 126.27 (C_{para}), 124.71 (C_{meta}), 123.08 (C_{meta}), 44.67 ($C(CH_3)_3$), 29.10 ($CHMe_2$), 29.06 ($C(CH_3)_3$), 28.70 ($CHMe_2$), 28.49 ($CH(CH_3)_2$), 27.90 ($CH(CH_3)_2$), 23.02 ($CH(CH_3)_2$), 22.39 ($CH(CH_3)_2$); $\delta_{119Sn}(C_6D_6)$ +2.97; m/z 573 (M^+), 539 ($M - Cl$).

Synthesis of $[^tBuC(NAr)_2]SnO^iPr$, 3

A solution of LiO^iPr (0.38 g, 5.79×10^{-3} mol) in 20 mL toluene was added dropwise to a solution of complex **2** (3.02 g, 5.26×10^{-3} mol) in toluene (15 mL) at −78 °C. After stirring

for 18 h at room temperature, the solvent was removed under reduced pressure and the product was extracted into pentane (20 mL). Recrystallisation from a saturated pentane solution at room temperature gave colourless crystals of [^{t}BuC(NAr)$_2$]SnO^{i}Pr, (1.60 g, 2.68 × 10^{-3} mol, 51% yield). Crystals suitable for X-ray diffraction were grown by allowing a saturated pentane solution to stand at room temperature for several days, (Found: C 64.40, H 8.37, N 4.79%; $C_{32}H_{50}N_2OSn$ requires C 64.33, H 8.44, N 4.69%); $\delta_H(C_6D_6)$ 7.15–7.02 (m, 6H, H_{meta}, H_{para}), 4.44 (sept, ^{1}H, $^3J_{HH}$ = 6.0 Hz, OC*H*Me$_2$), 3.96 (br sept, 2H, C*H*Me$_2$), 3.64 (br sept, 2H, C*H*Me$_2$), 1.43 (br d, 6H, CH(C*H*$_3$)$_2$), 1.37 (br d, 6H, CH(C*H*$_3$)$_2$), 1.31 (br d, 6H, CH(C*H*$_3$)$_2$), 1.26 (br d, 6H, CH(C*H*$_3$)$_2$), 1.25 (d, 6H, $^3J_{HH}$ = 6.0 Hz, OCH(C*H*$_3$)$_2$), 0.93 (s, 9H, C(C*H*$_3$)$_3$); $\delta_C(C_6D_6)$ 177.32 (^{t}Bu*C*(NAr)$_2$), 145.46 (C_{ortho}), 143.23 (C_{ortho}), 141.01 (C_{ipso}), 125.66 (C_{para}), 123.98 (C_{meta}), 123.17 (C_{meta}), 66.09 (O*C*HMe$_2$), 44.28 (*C*(CH$_3$)$_3$), 29.61 (OCH(*C*H$_3$)$_2$), 29.32 (C(*C*H$_3$)$_3$, 28.93 (*C*HMe$_2$), 28.56 (*C*HMe$_2$), 28.01 (CH(*C*H$_3$)$_2$), 27.66 (CH(*C*H$_3$)$_2$), 22.79 (CH(*C*H$_3$)$_2$), 22.38 (CH(*C*H$_3$)$_2$); $\delta_{119Sn}(C_6D_6)$ −28.58; *m*/*z* 598 (M$^+$), 538 (M − OCH(CH$_3$)$_2$).

Synthesis of [^{t}BuC(NAr)$_2$]SnNMe$_2$, 4

A suspension of LiNMe$_2$ (0.047 g, 0.917 × 10^{-3} mol) in toluene (30 mL) was added dropwise to a solution of complex **2** (0.501 g, 0.873 × 10^{-3} mol) in toluene (30 mL) at −78 °C. The reaction was allowed to stir for 18 h whilst warming to room temperature. The yellow solution was filtered and the filtrate concentrated under reduced pressure to give the crude product as a pale yellow solid in quantitative yield. Recrystallisation from a saturated heptane solution at −30 °C gave **4** as pale yellow crystals (0.291 g, 0.499 × 10^{-3} mol, 57% yield). Crystals suitable for X-ray crystallographic analysis were grown from a pentane solution at room temperature, (Found: C 63.74, H 8.42, N 7.09%; $C_{31}H_{49}N_3Sn$ requires C 63.93, H 8.48, N 7.21%); $\delta_H(C_6D_6)$ 7. 12–7.07 (m, 6H, H_{meta}, H_{para}), 3.84 (br sept, 2H, $^3J_{HH}$ = 6.7 Hz, C*H*Me$_2$), 3.71 (br sept, 2H, $^3J_{HH}$ = 6.7 Hz, C*H*Me$_2$), 3.26 (s, 6H, N(C*H*$_3$)$_2$), 1.33 (d, 12H, $^3J_{HH}$ = 6.9 Hz, CH(C*H*$_3$)$_2$), 1.29 (d, 6H $^3J_{HH}$ = 6.9 Hz, CH(C*H*$_3$)$_2$), 1.27 (d, 6H, $^3J_{HH}$ = 6.7 Hz, CH(C*H*$_3$)$_2$), 0.94 (s, 9H, C(C*H*$_3$)$_3$); $\delta_C(C_6D_6)$ 177.83 (^{t}Bu*C*(NAr)$_2$), 144.31 (C_{ortho}), 143.99 (C_{ortho}), 141.88 (C_{ipso}), 125.51 (C_{para}), 124.26 (C_{meta}), 123.47 (C_{meta}), 44.21 (*C*Me$_3$), 43.31 (N(*C*H$_3$)$_2$), 29.64 (C(*C*H$_3$)$_3$), 28.90 (*C*HMe$_2$), 28.56 (*C*HMe$_2$), 28.21 (CH(*C*H$_3$)$_2$), 26.19 (CH(*C*H$_3$)$_2$), 22.86 (CH(*C*H$_3$)$_2$); $\delta_{119Sn}(C_6D_6)$ +18.34; *m*/*z* 539 (M − N(CH$_3$)$_2$).

Synthesis of [^{t}BuC(NAr)$_2$]SnN(SiMe$_3$)$_2$, 5

Complex **5** was prepared in an analogous manner to **4** using 0.756 g [^{t}BuC(NAr)$_2$]SnCl (1.31 × 10^{-3} mol) and 0.231 g LiN(SiMe$_3$)$_2$ (1.38 × 10^{-3} mol). Recrystallisation from heptane afforded yellow crystals of [^{t}BuC(NAr)$_2$]SnN(SiMe$_3$)$_2$ (0.606 g, 0.864 × 10^{-3} mol, 66% yield), (Found: C 59.81, H 8.60, N 5.71%; $C_{35}H_{61}N_3Si_2Sn$ requires C 60.16, H 8.80, N 6.01%); $\delta_H(C_6D_6)$ 7.12–7.02 (m, 6H, H_{meta}, H_{para}), 3.65 (sept, 2H, $^3J_{HH}$ = 6.8 Hz, C*H*Me$_2$), 3.60 (sept, 2H, $^3J_{HH}$ = 6.8 Hz, C*H*Me$_2$), 1.45 (d, 6H, $^3J_{HH}$ = 6.8 Hz, CH(C*H*$_3$)$_2$), 1.37 (d, 6H, $^3J_{HH}$ = 6.9 Hz, CH(C*H*$_3$)$_2$), 1.31 (d, 6H, $^3J_{HH}$ = 6.8 Hz, CH(C*H*$_3$)$_2$), 1.27 (d, 6H, $^3J_{HH}$ = 6.8 Hz, CH(C*H*$_3$)$_2$), 0.96 (s, 9H, C(C*H*$_3$)$_3$), 0.07 (s, 18H, Si(C*H*$_3$)$_3$); $\delta_C(C_6D_6)$ 171.34 (^{t}Bu*C*(NAr)$_2$), 144.91 (C_{ortho}), 142.28 (C_{ipso}), 142.04 (C_{ortho}), 125.64 (C_{para}), 124.32 (C_{meta}), 123.79 (C_{meta}), 44.44 (*C*Me$_3$), 30.16 (C(*C*H$_3$)$_3$, 28.95 (*C*HMe$_2$), 28.81 (*C*HMe$_2$), 27.86 (CH(*C*H$_3$)$_2$), 26.47 (CH(*C*H$_3$)$_2$), 23.76 (CH(*C*H$_3$)$_2$), 23.41 (CH(*C*H$_3$)$_2$), 5.26 (Si(*C*H$_3$)$_3$); $\delta_{119Sn}(C_6D_6)$ +50.00; *m*/*z* 699 (M$^+$), 539 (M − N(Si(CH$_3$)$_3$)$_2$).

General polymerisation procedure

Toluene (10 mL) was added to an ampoule precharged with *rac*-LA (0.4041 g, 2.80 mmol) and **3**, **4** or **5** (0.0028 mmol). The reaction was immediately transferred to an oil-bath preheated to 60 °C and aliquots were sampled with time. The reaction was eventually quenched with 1 drop of methanol and monomer conversion was determined by ^{1}H NMR spectroscopy. After the solvent was removed under reduced pressure the residue was redissolved in a small volume of chloroform and the polymer was precipitated from excess cold acidic methanol and dried *in vacuo* for 18 h. The molecular weight and PDI were determined by gel permeation chromatography.

General procedure used for kinetic studies

All kinetic runs were carried out in a glovebox. Into a polymerisation ampoule containing *rac*-LA (0.4041 g, 2.80 mmol) an appropriate amount of toluene stock solution of **3** was added to give a 0.28 M solution of lactide with the desired [LA]$_0$: **3** ratio. At appropriate time intervals, 0.5 mL aliquots were removed and quenched with 1 drop of methanol and the conversion was determined by ^{1}H NMR spectroscopy.

Crystallography‡

Crystal data for 1. $C_{52}H_{74}N_4Sn$, M = 873.84, monoclinic, $P2/c$ (no. 13), a = 21.8742(6), b = 10.9039(3), c = 20.8390(5) Å, β = 97.598(2)°, V = 4926.8(2) Å^3, Z = 4 (two C_2-symmetric molecules), D_c = 1.178 g cm^{-3}, μ(Mo-Kα) = 0.555 mm^{-1}, T = 173 K, colourless prisms; 16 674 independent measured reflections (R_{int} = 0.032), F^2 refinement, R_1 = 0.076 for 15 788 independent, observed, absorption-corrected reflections [$|F_o| > 4\sigma(|F_o|)$, $2\theta_{max}$ = 65.2°], wR_2 = 0.176 (all data), 517 parameters.

Crystal data for 2. $C_{29}H_{43}N_2ClSn$, M = 573.79, monoclinic, $P2_1/n$, a = 9.5201(4), b = 16.9282(6), c = 17.8114(7) Å, β = 90.911(2)°, V = 2870.09(19) Å^3, Z = 4, D_c = 1.328 g cm^{-3}, μ(Mo-Kα) = 1.002 mm^{-1}, T = 150 K, colourless blocks; 6978 independent measured reflections (R_{int} = 0.017), F^2 refinement, R_1 = 0.024 for 6069 independent, observed, absorption-corrected reflections [$|F_o| > 4\sigma(|F_o|)$, $2\theta_{max}$ = 58.0°], wR_2 = 0.058 (all data), 309 parameters.

Crystal data for 3. $C_{32}H_{50}N_2OSn$, M = 597.43, orthorhombic, $Pbca$, a = 18.3898(5), b = 17.9716(4), c = 19.1257(5) Å, V = 6320.9(3) Å^3, Z = 8, D_c = 1.256 g cm^{-3}, μ(Mo-Kα) = 0.833 mm^{-1}, T = 150 K, colourless blocks; 7878 independent measured reflections (R_{int} = 0.020), F^2 refinement, R_1 = 0.025 for 6329 independent, observed, absorption-corrected reflections, [$|F_o| > 4\sigma(|F_o|)$, $2\theta_{max}$ = 58.2°], wR_2 = 0.066 (all data), 338 parameters.

Crystal data for 4. $C_{31}H_{49}N_3Sn$, M = 582.42, triclinic, $P\bar{1}$, a = 10.0495(9), b = 11.0334(10), c = 15.5989(14) Å, α = 99.131(2)°, β = 107.283(2)°, γ = 106.213(2)°, V = 1529.8(2) Å^3, Z = 2, D_c = 1.264 g cm^{-3}, μ(Mo-Kα) = 0.857 mm^{-1}, T = 150 K, pale yellow needles; 6970 independent measured reflections (R_{int} = 0.021),

$R_1 = 0.028$ for 6286 independent, observed, absorption-corrected reflections [$|F_o| > 4\sigma(|F_o|)$, $2\theta_{max} = 57.7°$], $wR_2 = 0.070$ (all data), 329 parameters.

Crystal data were measured on Oxford Diffraction Xcalibur 3 (**1**) and Bruker AXS SMART 1000 CCD (**2**, **3** and **4**) diffractometers with Mo-Kα ($\lambda = 0.71073$ Å) radiation, using ω-scans with narrow frames. Lp and absorption corrections were applied based on symmetry equivalent and repeated measurements. All structures were solved by direct methods with non-H atoms refined anisotropically and H atoms included in a riding model. Anisotropic displacement parameter restraints were applied to ^{i}Pr and ^{t}Bu C atoms in **3**.

Programs: Oxford Diffraction CrysAlis CCD[42] and Bruker SMART[43] (diffractometer control), Oxford Diffraction CrysAlis RED[42] and SAINT[43] (data reduction), SHELXTL[44] (solution and refinement) and local programs.

CCDC reference numbers 645832–645835.

For crystallographic data in CIF or other electronic format see DOI: 10.1039/b706663e.

Acknowledgements

The authors express their gratitude to the Royal Thai Government for a studentship (N. N.) and the Engineering and Physical Sciences Research Council (UK) for a studentship (S. H. D.).

References

1 A. H. Tullo, *Chem. Eng. News*, 2002, **80**, 13.
2 A. J. Nijenhuis, D. W. Grijpma and A. J. Pennings, *Macromolecules*, 1992, **25**, 6419.
3 B. J. O'Keefe, M. A. Hillmyer and W. B. Tolman, *J. Chem. Soc., Dalton Trans.*, 2001, 2215.
4 O. Dechy-Cabaret, B. Martin-Vaca and D. Bourissou, *Chem. Rev.*, 2004, **104**, 6147.
5 V. C. Gibson, and E. L. Marshall, in *Comprehensive Coordination Chemistry II*, ed. J. A. McCleverty and T. J. Meyer, Elsevier, Oxford, UK, 2003, vol. 9, ch. 1, pp. 36–52.
6 G. Schwach, J. Coudane, R. Engel and M. Vert, *J. Polym. Sci., Part A: Polym. Chem.*, 1997, **35**, 3431.
7 H. R. Kricheldorf, *Macromol. Symp.*, 2000, **153**, 55.
8 H. R. Kricheldorf, I. Kreiser-Saunders and C. Boettcher, *Polymer*, 1995, **36**, 1253.
9 A. Kowalski, A. Duda and S. Penczek, *Macromolecules*, 2000, **33**, 689.
10 H. R. Kricheldorf, M. Berl and N. Scharnagl, *Macromolecules*, 1988, **21**, 286.
11 A. P. Dove, V. C. Gibson, E. L. Marshall, A. J. P. White and D. J. Williams, *Chem. Commun.*, 2001, 283.
12 A. P. Dove, V. C. Gibson, E. L. Marshall, H. S. Rzepa, A. J. P. White and D. J. Williams, *J. Am. Chem. Soc.*, 2006, **128**, 9834.
13 M. Cheng, A. B. Attygalle, E. B. Lobkovsky and G. W. Coates, *J. Am. Chem. Soc.*, 1999, **121**, 11583.
14 B. M. Chamberlain, M. Cheng, D. R. Moore, T. M. Ovitt, E. B. Lobkovsky and G. W. Coates, *J. Am. Chem. Soc.*, 2001, **123**, 3229.
15 M. H. Chisholm, J. C. Huffman and K. Phomphrai, *J. Chem. Soc., Dalton Trans.*, 2001, 222.
16 M. H. Chisholm, J. Gallucci and K. Phomphrai, *Inorg. Chem.*, 2002, **41**, 2785.
17 M. H. Chisholm, J. Gallucci and K. Phomphrai, *Chem. Commun.*, 2003, 48.
18 M. H. Chisholm, J. Gallucci and K. Phomphrai, *Inorg. Chem.*, 2004, **43**, 6717.
19 V. C. Gibson, E. L. Marshall, D. Navarro-Llobet, A. J. P. White and D. J. Williams, *Dalton Trans.*, 2003, 4321.
20 J. Barker and M. Kilner, *Coord. Chem. Rev.*, 1994, **133**, 219.
21 F. T. Edelmann, *Coord. Chem. Rev.*, 1994, **137**, 403.
22 R. T. Boeré, V. Klassen and G. Wolmershäusen, *J. Chem. Soc., Dalton Trans.*, 1998, 4147.
23 U. Kilimann, M. Noltemeyer and F. T. Edelmann, *J. Organomet. Chem.*, 1993, **443**, 35.
24 Y. Zhou and D. S. Richeson, *J. Am. Chem. Soc.*, 1996, **118**, 10850.
25 P. B. Hitchcock, M. F. Lappert and M. Layh, *J. Chem. Soc., Dalton Trans.*, 1998, 3113.
26 S. R. Foley, Y. Zhou, G. P. A. Yap and D. S. Richeson, *Inorg. Chem.*, 2000, **39**, 924.
27 K. B. Aubrecht, M. A. Hillmyer and W. B. Tolman, *Macromolecules*, 2002, **35**, 644.
28 F. Antolini, P. B. Hitchcock, A. V. Khvostov and M. F. Lappert, *Can. J. Chem.*, 2006, **84**, 269.
29 A. Xia, H. M. El-Kaderi, M. J. Heeg and C. H. Winter, *J. Organomet. Chem.*, 2003, **682**, 224.
30 M. P. Coles, D. C. Swenson, R. F. Jordan and V. G. Young, *Organometallics*, 1997, **16**, 5183.
31 S. P. Green, C. Jones, P. C. Junk, K.-A. Lippert and A. Stasch, *Chem. Commun.*, 2006, 3978.
32 S. R. Foley, G. P. A. Yap and D. S. Richeson, *J. Chem. Soc., Dalton Trans.*, 2000, 1663.
33 Y. Zhou and D. S. Richeson, *Inorg. Chem.*, 1997, **36**, 501.
34 Y. Q. Ding, H. W. Roesky, M. Noltemeyer, H. G. Schmidt and P. P. Power, *Organometallics*, 2001, **20**, 1190.
35 S. Penczek, A. Duda and R. Szymanski, *Macromol. Symp.*, 1998, **132**, 441.
36 T. Ouhadi, A. Hamitou, R. Jérôme and P. Teyssié, *Macromolecules*, 1976, **9**, 927.
37 P. Dubois, C. Jacobs, R. Jérôme and P. Teyssié, *Macromolecules*, 1991, **24**, 2266.
38 B. M. Chamberlain, B. A. Jazdzewski, M. Pink, M. A. Hillmyer and W. B. Tolman, *Macromolecules*, 2000, **33**, 3970.
39 H. Ma and J. Okuda, *Macromolecules*, 2005, **38**, 2665.
40 H. R. Kricheldorf, C. Boettcher and K. U. Tönnes, *Polymer*, 1992, **33**, 2817.
41 P. Foley and M. Zeldin, *Inorg. Chem.*, 1975, **14**, 2264.
42 *CrysAlis CCD and RED software*, Oxford Diffraction Ltd., Abingdon, Oxon, UK, 2004.
43 *SMART and SAINT software for CCD diffractometers*, Bruker AXS Inc., Madison, WI, USA, 2001.
44 G. M. Sheldrick, *SHELXTL user manual*, version 6.10, Bruker AXS Inc., Madison, WI, USA, 2000.